Neutrophils rapidly migrate via lymphatics after Mycobacterium bovis BCG intradermal vaccination and shuttle live bacilli to the draining lymph nodes

Valérie Abadie, Edgar Badell, Patrice Douillard, Danielle Ensergueix, Pieter J. M. Leenen, Myriam Tanguy, Laurence Fiette, Sem Saeland, Brigitte Gicquel, Nathalie Winter

Neutrophils rapidly migrate via lymphatics after *Mycobacterium bovis* BCG intradermal vaccination and shuttle live bacilli to the draining lymph nodes

Short title : Neutrophils shuttle BCG to the DLN via lymphatics

Valérie Abadie[1], Edgar Badell[1], Patrice Douillard[2], Danielle Ensergueix[1], Pieter J. M. Leenen[3], Myriam Tanguy[4], Laurence Fiette[4], Sem Saeland[2], Brigitte Gicquel[1] and Nathalie Winter[1]

From the [1] Mycobacterial Genetics Unit and the [4]Laboratory of Histotechnology and Pathology, Institut Pasteur, Paris, France; [2]Laboratory for Immunological Research, Schering Plough Dardilly, France; and the [3]Department of Immunology, Erasmus Medical Center, Rotterdam, the Netherlands

This work was supported by grants from European Economic Community (QLRT-PL1999-00228 and ICA4-1999-40006) and the Agence Nationale de Recherches contre le SIDA (V.A)

Corresponding author : Nathalie Winter , Mycobacterial Genetics Unit, Institut Pasteur, 25 rue du Docteur Roux, 75724 Paris Cedex 15, France, Phone +33 1 40 61 35 99, Fax : +33 1 45 68 88 43, e.mail: nwinter@pasteur.fr

Scientific section designation: PHAGOCYTES

Abstract

The early innate response after *Mycobacterium bovis* BCG vaccination is poorly characterized, but probably decisive for subsequent protective immunity against tuberculosis. Therefore, we vaccinated mice with fluorescent BCG strains in the ear dorsum, as a surrogate of intradermal vaccination in humans. During the first three days, we tracked BCG host cells migrating out of the dermis to the auricular draining lymph nodes (ADLN). Resident skin dendritic cells (DCs) or macrophages did not play a predominant role in early BCG capture and transport to ADLN. The main BCG host cells rapidly recruited both in the dermis and ADLN were neutrophils. Fluorescent green or red BCG strains injected into non-overlapping sites were essentially sheltered by distinct neutrophils in the ADLN capsule indicating that neutrophils had captured bacilli in peripheral tissue and transported them to the lymphoid organ. Strikingly, we observed BCG-infected neutrophils in the lumen of lymphatic vessels by confocal microscopy on ear dermis. Fluorescent-labeled neutrophils injected into the ears, accumulated exclusively into the ipsilateral ADLN capsule after BCG vaccination. Thus, we provide *in vivo* evidence that neutrophils, like DCs or inflammatory monocytes, migrate via afferent lymphatics to lymphoid tissue and can shuttle live microorganisms.

Introduction

Mycobacterium bovis BCG is the only available vaccine against tuberculosis (TB), a major public health problem. Being included in the WHO Expanded Program for Immunization, BCG is one of the most widely administered vaccines. It confers high levels of protection against disseminated forms of TB, particularly severe in children, but its efficacy against pulmonary TB in adults is estimated to be only 50 percent [1] and varies widely between different geographic areas and populations. Thus more efficient vaccines against TB are urgently needed. There are reasons to believe that such vaccines could be based on BCG. Therefore, a better understanding of the immune response induced by BCG could help to design better strategies on a rational basis. Today, BCG vaccination is almost exclusively administered intradermally or percutaneously [2]. Early events taking place after BCG vaccination that will strongly impact on the adaptive immune response are poorly characterized. For example, it is unknown how BCG travels from the injection site to draining lymph nodes (DLN) and which host cells could be involved in this early process. Mononuclear phagocytes such as epidermal Langerhans cells (LCs), dermal macrophages and DCs are ideally located to capture microorganisms entering skin. Due to their migratory capacity, DCs shuttle pathogens such as HIV [3] or *Leishmania major* [4] to DLN. Bacterial dissemination from gut to mesenteric DLN occurs via infected DCs after ingestion of *Salmonella* [5] or *Listeria* [6]. Peripheral tissue DCs are not the only cells at play in bridging innate and acquired immunity to pathogens. Soon after an inflammatory stimulus, blood monocytes are recruited to the injured tissue from which they can migrate via afferent lymph towards DLN. There, monocytes acquire a DC phenotype [7] and prime the T-cell response [8]. During systemic infection with *Listeria monocytogenes*, blood monocytes are able to shuttle bacteria into the brain [9]. Thus, it is also plausible that inflammatory monocytes could transport

pathogens from peripheral tissue to DLN, although recent work suggests that, after *Salmonella typhimurium* injection into the skin, local inflammation impairs their migration and conversion to DCs in the DLN [10].

Given the decisive impact of innate events taking place after BCG vaccination on the ensuing adaptive immune response, we decided to analyze them in mice injected into a strictly dermal site, the ear dorsum. Taking advantage of a fluorescent rBCG-*egfp* strain, cells carrying BCG were characterized from skin explants and auricular DLN (ADLN) at early time-points after BCG vaccination. Contrary to our expectations, resident skin mononuclear phagocytes did not play a predominant role in BCG capture and transport to secondary lymphoid organs. We observed that neutrophils, that were the first cells recruited into the ear dermis and captured BCG, also massively infiltrated the ADLN where they represented the main primary host cells for BCG. Neutrophils carrying fluorescent bacilli were detected inside skin lymphatic vessels. Upon BCG vaccination, green or red fluorescent labelled neutrophils injected into left or right ear migrated exclusively to the ipsilateral DLN. Together our data support the concept that neutrophils leave an inflamed site via afferent lymphatics, migrate to the secondary lymphoid organ and participate in the transport of live microorganisms.

Materials and methods

Animals

Female 6-12 weeks C57BL/6 mice (Centre d'Elevage Janvier, Le Gesnet-Saint-L'Isle, France) were housed in our animal care facility under specific pathogen free conditions.

Bacterial strain, immunizations and CFU determination

Mycobacterium bovis BCG Pasteur 1173P2 was transformed with Ms6 derived integrative vectors [11] expressing either the *Aequoria victoria egfp* gene to obtain green fluorescent BCG strain Myc 409 or the *ds-red1* gene cut from plasmid pGMDs3 [12] to obtain red-fluorescent BCG strain Myc 3305. Strains were grown as dispersed cultures in Beck medium and harvested at log-phase to freeze aliquots at –80°C [13]. 10^6 CFU from frozen titered stocks were inoculated intradermally into each mouse ear dorsum under 10 µl. For CFU determination, each ear and ADLN from five mice were collected and homogenized. Viable bacteria were counted after plating onto solid 7H11 medium enriched with OADC (BD Microbiology Systems, Sparks, MD).

Skin explant cultures and preparation of ADLN cell suspensions

At different time points after BCG-*egfp* injection into the ear dorsum, mice were euthanized and ears were surgically removed. Control mice inoculated with 10 µl of Beck medium were processed the same way. Dorsal and ventral halves were split and layered on RPMI 1640 supplemented with 10% FCS (Dominique Dutscher, Brumath, France), HEPES (100 mM) and penicillin (100 µg/ml). After 24 h at 37°C, ear skin explant migrating cells from eight mice were pooled and filtered through a 70 µm nylon mesh before antibody staining. ADLN cells were dissociated from the matrix by a 25 min incubation at 37°C with 1 mg/ml collagenase D and 40

µg/ml DNAseI (Roche-Diagnostics, Mannheim, Germany) in RPMI. Cells were filtered through a 70 µm nylon mesh and layered on a Histodenz gradient (Sigma-Aldrich, St-Louis, MO) prepared in RPMI 10% FCS. Low density cells -composed mainly of macrophages, granulocytes and DCs- were collected and washed in PBS. In some experiments, DCs were enriched by positive immunomagnetic selection using anti-CD11c coated beads according to the manufacturer's recommendations (MACS, Miltenyi Biotec, Bergisch Gladbach, Germany) before antibody staining.

Flow cytometry and sorting

Conjugated antibodies against CD11b-PE, biotin or APC (clone M1/70), I-A/I-E-biotin, (clone 2G9), Ly-6G-PE (clone 1A8), CD11c-PE or APC (clone HL3), were purchased from BD Pharmingen (San Diego, CA) and anti-F4/80 (clone A3-1) was purchased from Serotec (Oxford, UK). Biotinylated mAb 929F3 was used for intracytoplasmic Langerin/CD207 staining of LCs [14]. Isotype controls were all from BD Pharmingen. After a 20 min incubation with purified anti-CD16/32 mAb (clone 2.4G2, BD Pharmingen), surface staining was performed in PBS-FACS (PBS, 5% FCS, 0.05% sodium azide) supplemented with 0.1 % total mouse serum. For intracytoplasmic Langerin detection, cells were permeabilized with Fix/Perm^{TM} kit (BD Pharmingen) before incubation with mAb 929F3. Antibodies were incubated for 30 min followed by two washes in PBS-FACS. When biotinylated antibodies were used, the secondary reagent was streptavidin-PerCP-Cy5 (BD Pharmingen). Fluorescence was analyzed on a total of 3.10^4 cells per sample using FACSCalibur and CellQuest Pro software (BD Biosciences).

Morphological characterization of FACS-sorted neutrophils

Twenty-four hours after BCG inoculation, ADLN or skin explant cells were isolated. $CD11b^+$ cells were enriched by positive selection with immunomagnetic beads using the MACS system (Miltenyi) and $CD11b^+$ $EGFP^+$ cells were then sorted on a FACSCalibur (BD Biosciences). 2 x 10^5 cells were either cytocentrifuged onto slides, air-dried and then fixed with methanol, or were allowed to adhere onto polylysine (Sigma-Aldrich)-coated coverslips for 30 min and then fixed for 20 min in PBS-2% paraformaldehyde. Cytocentrifuged slides were colored with May-Grünwald-Giemsa and coverslips were stained with anti-Ly-6G followed by Alexa Fluor® 594 goat anti-rat IgG (Molecular Probes, Eugene, OR). To assess nuclear morphology, coverslips were incubated 5 min at room temperature with DAPI (Molecular Probes) and examined under UV fluorescence microscope.

Immunofluorescence and immunohistochemistry on tissue sections

Frozen tissues were cryosectioned (5-µm thick sections) and sections were fixed for 10 min in acetone. Slides were sequentially rehydrated for 10 min in PBS, treated for 30 min at room temperature with blocking agent (DuPont NEN, Boston, MA) and incubated for 2h at room temperature with rat anti-Langerin/CD207 929F3, ER-MP23 directed against the mouse Macrophage Galactose N-acetylgalactosamine Lectin (MGL) / asialoglycoprotein receptor (ASGPR), anti-Ly-6G, anti-CD4 (clone RM4-5), or anti-CD8 (clone 53-6.7). Slides were then incubated 45 min at room temperature with secondary antibody goat anti-rat IgG-Alexa fluor® 594, 488, or 633 (Molecular Probes). For anti-CD11c staining, slides were rehydrated in PBS-1%BSA for 10 min and endogenous biotin was blocked using the Avidin/Biotin Blocking Kit (Vector laboratories, Burlingame, CA) for 30 min at room temperature. Thereafter, slides were

incubated with biotin conjugated anti-CD11c for 2 h followed by Texas-Red-conjugated streptavidin (Molecular Probes) for 45 min at room temperature. After three washes in PBS, slides were mounted with Fluoromount-G (SouthernBiotech Associates, Birmingham, AL). Slides were analyzed with fluorescence microscope (Axioskop, Zeiss, Germany) equipped with an image processing and analysis system Advanced Quips (Leica Camera AG, Solms, Germany) or confocal microscope equipped with a blue laser diode 405 nm, an Ar laser 488 nm, and a HeNe laser 543 nm and the software LSM 510 V3.2 (Zeiss). Detection of lymphatic vessels in ear dermis was performed thanks to anti-Lyve-1 antibody [15] generously given by Dr David Jackson (John Radcliffe Hospital, Oxford, UK). For immunohistochemistry on transversal sections, ears were incubated for 2 days at 4°C in PBS-4% paraformaldehyde. They were then dried by serial washes in baths ranging from 70 to 100% ethanol and 100% xylene. Three final washes were performed in 100% paraffin at 60°C. Sections of 5-µm thickness were transferred onto glass slides. Paraffin was removed by incubating the slides twice for 5 min in xylene, and then twice for 1 min in 100% ethanol. Slides were dried and rehydrated for 20 min in PBS. Endogenous peroxidases were inactivated by a 20 min incubation in PBS-1%H_2O_2. After three washes in PBS and incubation for 30 min with blocking Agent (DuPont NEN), slides were incubated with anti-Lyve-1 overnight, then 30 min with secondary anti-rabbit-HRP using the Envision™+System HRP Rabbit from Dako (Via Real, CA). Peroxidase activity was revealed with AEC (AEC Substrate kit for peroxidase, Vector Laboratories). Cells were either counter-colored with hematoxylin (Shandon), or incubated with anti-Ly-6G for 1h, followed by 1h incubation with biotinylated rat Ig (Dako), and 1h incubation with AP-streptavidin (Dako). AP activity was revealed with a Fast Blue substrate-chromogen system (Sigma-Aldrich). Slides were preserved in aquamount (BDH, Poole Dorset, UK). For immunofluorescence on whole dermis,

ear dorsal halves were incubated in 0.5 M phosphate buffered ammonium thiocyanate for 30 min at 37°C. Epidermis were peeled off and dermis were fixed in PBS-2% paraformaldehyde. After three washes with PBS, dermis were incubated with anti-Lyve-1 antibody overnight at 4°C. The following 30 min incubation were serially performed : goat anti-rabbit IgG-Alexa fluor® 594 (Molecular Probes), anti-Ly-6G (BD) and goat anti-rat IgG-Alexa fluor® 633 (Molecular Probes). Slides were analyzed with confocal microscope as described above.

Bone-marrow neutrophil purification, fluorescent labeling and in vivo trafficking

Bone-marrow cells from four mice were harvested in PBS, 0.5% FCS. For depletion of lymphocytes, monocytes and DCs, cells were incubated with a cocktail of mAbs, anti-F4/80, anti-I-A/I-E, anti-CD4 anti-CD8, anti-B220 (clone RA3-6B2) and anti-CD11c all biotin-conjugated and used at 10 µg/ml (all from BD Pharmingen, except anti F4/80 from Serotec). After 15 min incubation, avidin-coated magnetic beads (MACS, Miltenyi) were added for 15 min. This negative selection was followed by positive selection by incubating cells 15 min with purified anti-Ly-6G and then 15 min with anti-rat IgG-coated magnetic beads (MACS, Miltenyi). More than 95% pure neutrophils were obtained as assessed by microscopy after May-Grünwald-Giemsa staining. Viability by trypan blue exclusion was 98%. For *in vivo* tracking experiments, neutrophils were incubated with the green fluorescent dye CFSE (Molecular Probes) or the red fluorescent dye PKH26 (Sigma-Aldrich) according to the manufacturer's protocol. Cells (10^6/ear) were injected in the ear dorsum with or without concomittant injection of 10^6 CFUs of wild type BCG. Four hours later each ear and ADLN was frozen and embedded in OCT compound (Fischer Diagnostcis, Middleton, VA). Frozen tissues were cryosectioned (5-µm thick sections), collected

on Superfrost slides (Fischer Diagnostics), air-dried and observed under a fluorescence microscope as described above.

Results

Intradermal inoculation of BCG in mouse ear rapidly leads to bacilli tranfer to ADLN

In order to study cell migration that take place early after intradermal BCG vaccination, we have used a model of BCG inoculation in mouse ear, a site allowing injection strictly into the dermis and excluding the involvement of subcutaneous connective tissue [16]. We first quantified bacterial multiplication in the ear and the ADLN after vaccination with 10^6 CFUs of BCG (Figure 1). The majority of the injected BCG was recovered from the ears at 4 hours post injection (hpi) and the bacterial load only slightly declined over the next 7 days. At 14 days after injection, a more important reduction of the bacterial load was observed in the ear, probably corresponding to the onset of the adaptive immune response. In the ADLN, approximately 1% of the injected bacilli (10^4 CFUs) were recovered as soon as 4 hpi and this BCG load was stably maintained over the next 14 days. Thus, the model of BCG intradermal inoculation in C57/BL6 mouse ear leads to rapid tranfer of live bacilli into the ADLN where they can persist for at least two weeks.

DCs are minimally associated with BCG at the vaccination site and in the ADLN

In vivo, LCs from the epidermis and DCs from the dermis migrate to the DLN very shortly upon inflammatory stimulation. This situation can be mimicked *in vitro* by the skin explant culture method where cells migrating out of skin can be analyzed after 24 hours incubation in medium [17]. In order to track BCG-infected DCs crawling out of skin, we performed ear skin explant cultures from 4 to 72 hours after auricular injection of BCG-*egfp*. Throughout the kinetics, 19 to 48% from all skin explant cells were $EGFP^+$ i.e. BCG-infected (Figure 2A). Among them, remarkably low numbers –at most 3% - stained positive for CD11c, the most widely distributed mouse DC

marker indicating that rare emigrant DCs carried BCG. In accordance, BCG was generally not associated with $CD11c^+$ DCs in the dermis as observed after immunofluorescence on ear skin sections (Figure 2B). We also analyzed LCs and BCG association by means of anti-CD207 (Langerin) antibody 929F3 [14]. At 12 and 72 hpi between 19 and 5 % of the total skin explants emigrant $CD11c^+$ cells were identified as LCs. Among all skin emigrant LCs, a maximum of 4% carried BCG and no Langerin-BCG colocalization could be observed in ear skin sections (Supplemental Figure S1). Thus, although rare skin emigrant DCs carrying BCG could be observed by flow cytometry, they accounted for a minor proportion of total BCG-host cells.

We next stained ear sections with ER-MP23, an antibody directed against mMGL1/2 (murine macrophage galactose/N-acetylgalactosamine-specific C-type lectin/DC asialoglycoprotein receptor) a receptor largely distributed on mononuclear phagocytes that populate mouse skin [18]. At 4 hpi or 72 hpi, we rarely detected $ER\text{-}MP23^+$ cells carrying BCG (Figure 2B). Taken together, our data indicate that resident skin mononuclear phagocytes, including LCs, dermal DCs and macrophages, are not main cells for early BCG uptake at the vaccination site.

As BCG transfer from the injection site to the ADLN was found to occur rapidly, we assessed whether BCG-loaded DCs could be detected in the ADLN. Thus, we analyzed $CD11c^+$ cells in ADLN from 4 to 72 hpi (Figure 3A). A maximum of 1% of $CD11c^+EGFP^+$ cells were observed indicating that CD11c+ cells were not predominant host cells for BCG in the ADLN. These results were supported by immunofluorescence on ADLN sections, where colocalization of $CD11c^+$ cells and BCG was only rarely observed at 72 hpi (Figure 3B).

To analyze if BCG loaded LCs could be detected in ADLN, $CD11c^+$ cells were enriched by magnetic selection at 12 and 72 hpi and flow cytometry was performed after straining with anti-CD207. Among the $CD11c^+$ $CD207^+$ LCs, none were associated with BCG and no colocalization

of CD207+ cells with BCG could be observed by immunohistochemistry on ADLN sections (Supplemental Figure S2). Together these results confirm that only a minor proportion of skin DCs, including epidermal LCs, is involved in early BCG transport from skin to ADLN.

Neutrophils are rapidly recruited at the site of inoculation and in ADLN where they represent the main early BCG host cells

Since we observed that mononuclear phagocytes only accounted for a minor fraction of $EGFP^+$ cells, thus harboring bacteria, in skin and ADLN following BCG inoculation, we further characterized the infected cells migrating out of skin explants. As soon as 4 hours post BCG-injection, a significant proportion of emigrants was carrying $EGFP^+$ bacteria and was $CD11b^+$ (Figure 4A). Their frequency among skin emigrants remained high through 72 hpi. These cells were further characterized as $CD11b^+$, $Ly\text{-}6G^+$, $F4/80^-$ and $MHCII^-$ (Figure 4B) suggesting that they were neutrophils. After flow cytometry sorting, the $EGFP^+$ cells displayed characteristic polylobed nuclei, which confirmed that the BCG-infected cells crawling out of skin were mainly neutrophils (Figure 4C). The localization of incoming neutrophils at the vaccination site was then analyzed by immunofluorescence using anti-Ly-6G [19] as a neutrophil specific marker, and not anti-Gr1 which detects both neutrophils and mononuclear cells (Figure 4D). From 4 to 72 hpi, neutrophils massively invaded the ear where they mostly colocalized with BCG. Interestingly, neutrophils remained focused around the bacilli over time suggesting a role in limiting BCG spread outside of the injection site. Until 72 hpi, neutrophils were the main dermal cells loaded with bacilli. Both high EGFP fluorescence and CFU counts at these time points showed that the neutrophils did not efficiently clear BCG from the dermis.

In the ADLN, twenty four hours following BCG-*egfp* inoculation, $EGFP^+$ cells were phenotyped by flow cytometry as $CD11b^{hi}$, $Ly\text{-}6G^{hi}$, $F4/80^-$ and MHC $classII^-$ indicating that most BCG-infected cells in the ADLN were neutrophils (Figure 5A). To confirm this surprising observation, ADLN $CD11b^+$ cells -including macrophages, some DC subsets and neutrophils- were magnetically enriched and $EGFP^+/CD11b^+$ cells were sorted by flow cytometry. The majority of BCG-loaded cells stained positive for Ly-6G and displayed the characteristic polylobed nuclei of neutrophils (Figure 5B). Neutrophil and BCG ($EGFP^+$) influx into the ADLN were then analyzed by immunofluorescence with anti-Ly-6G (Figure 5C). As early as 4 hpi, neutrophils infiltrated the ADLN capsule, and at 12 hpi sinuses were filled with $Ly\text{-}6G^+$ cells. By 72 hpi, neutrophils started to disappear from the ADLN. BCG and neutrophil colocalization was observed by confocal microscopy whereby green BCG bacilli were detected inside the cytoplasm of neutrophils surface-stained with anti-Ly-6G (Figure 5C, 12h).

Infected neutrophils leave the skin via lymphatic vessels after BCG vaccination and shuttle bacilli to the ADLN

We next asked where BCG-loaded neutrophils observed in the ADLN acquired bacilli. Indeed, our data suggested two possible pathways : i) bacilli mainly enter the ADLN capsule as free particles subsequently phagocytosed by neutrophils or, ii) phagocytosis occurs in the skin, and loaded neutrophils subsequently carry BCG to the ADLN. To address this question, we injected green fluorescent BCG-*egfp* and red fluorescent BCG-*dsred* into close but distinct sites of one ear dorsum. We reasoned that if bacilli mainly entered the ADLN capsule as free particles to be phagocytosed locally, then neutrophils carrying both red and green bacilli should mainly be observed. On the contrary, if neutrophils acquired bacilli in the periphery before migrating to the

ADLN, then cells carrying either red or green fluorescent BCG should be detected. Four hours following injection, ADLN cryosections containing a significative amount of green and red bacilli were selected and neutrophils were surface-stained with anti-Ly-6G. Seven different fields in each of these representative cryosections were scanned under a confocal microscope (Figure 6A). Individual Ly-6G$^+$ cells colocalized with either green or red bacilli, or with both strains were scored and averaged. After injection of red and green BCG in two distinct sites, we counted 75% +/- 8% of neutrophils colocalizing exclusively with red or green bacilli. Thus, a predominant proportion of infected neutrophils observed under the capsule acquired BCG in the periphery before migrating to the ADLN.

To confirm that BCG-infected neutrophils can enter skin lymphatics to migrate to the ADLN, ear cryosections were labeled four hours after BCG injection with antibody against Lyve-1, a molecule specifically expressed in lymphatic endothelium [15]. After hematoxylin counter-staining we observed that, close to the injection site, neutrophils characterized by their polylobed nucleus, were present in the lymphatic vessel lumen (Figure 6B). Phenotype and localization of such neutrophils was further confirmed by anti-Ly-6G and anti-Lyve-1 costaining (Figure 6B). After removing the epidermis, we stained the dermis with anti-Lyve-1 to observe longitudinal lymphatic vessels by confocal microscopy. Neutrophils, surface-stained with anti Ly-6G, were detected inside the lumen of lymphatics and contained intracellular BCG (EGFP$^+$) (Figure 6C). Thus, BCG-infected neutrophils were observed inside skin lymphatic vessels in the injection site vicinity confirming their capacity to shuttle live bacilli from skin to ADLN.

Fluorescent-labeled neutrophils injected into the ear accumulate in ipslateral ADLN after BCG administration

The migratory capacity of tissue resident DCs has been largely described. More recently, monocytes recruited to tissues upon inflammation have been shown to retro-transmigrate to the DLN [7,8]. To our knowledge, neutrophil trafficking from peripheral tissue to DLN via lymphatics has not been reported. To confirm this pathway, neutrophils were purified from syngeneic mouse bone marrow after anti-Ly-6G labeling and magnetic sorting. Neutrophils thus obtained (> 95% purity) were labeled *in vitro* with one of the two fluorescent dyes CFSE (green fluorescence) or PKH26 (red fluorescence) and were reinjected concomitantly with 10^6 CFUs of wild-type BCG into the left or right ear dorsal face, respectively. Four hours later, accumulation of green fluorescent neutrophils was observed in the subcapsular region of the LN draining the left ear and red fluorescent neutrophils were found to infiltrate the right ADLN (Figure 7A). No red fluorescent cells were observed in contralateral left ADLN and no green fluorescent cells were detected in the right ADLN. Thus, migration was restricted to the ipsilateral regional LN, which confirmed that neutrophils had reached the ADLN via afferent lymphatics and not via the systemic circulation.

Since the secondary lymphoid organ is a privileged site where the adaptive immune response takes place, we further analyzed the distribution of neutrophils in the ADLN. At 12 hpi, neutrophils that invaded the sinuses of the ADLN reached the paracortex and contacted T cells and CD11c+ DCs (Figure 7B), suggesting that neutrophils may play a role in antigen delivery.

Discussion

Gaining a better understanding of how BCG induces anti-mycobacterial immune responses could be of great benefit for improved vaccine development against tuberculosis. Today, BCG is the most widely administered live vaccine. It is injected almost exclusively intradermally, in sites known to be rich in professional antigen presenting cells. However, nothing is known about the role of skin cells in the onset of the immune response. We decided to characterize the early immune events induced locally and in the LN draining the BCG injection site using the mouse ear as a surrogate model of intradermal vaccination. We first determined if professional antigen-presenting cells populating the skin were involved in BCG uptake and transport from the vaccination site to the DLN. Skin or mucosal DCs, and especially LCs, which reside in epithelia, have been described to transport microorganisms to the DLN and help to establish persistent infection [4,20]. However, after inoculation of BCG in the ear dorsum, we did not detect BCG-infected LCs in the ADLN indicating that these cells are not predominantly involved in early BCG capture and transport. In this context, the role of LCs in shuttling Herpes Simplex Virus-2 [21] or *Leishmania major* [22], from the injection site to the DLN has recently been ruled out. Only on occasions, between 4 and 72 hpi, did we detect conventional $CD11c^+$ DCs carrying BCG in ADLN. Skin-derived DCs that reside in cutaneous LN are the first to acquire lymph-borne antigens inoculated into the mouse dermis [23]. Because BCG-loaded DCs, in the dermis or crawling out of skin explants, were barely observed at these time-points, we favor the idea that the rare early BCG-infected DCs in ADLN had captured live bacilli *in situ* rather than in the periphery. However, since BCG persisted in skin for at least 14 days, we do not rule out that resident DCs transported BCG to regional DLN after the first three days following inoculation, during later migration waves. Inflammatory blood-borne monocytes are able to shuttle *Listeria* [9]

into the brain. As these cells can also retro- transmigrate from tissue to LN via afferent lymph [7,8], they were also likely candidates to shuttle BCG to regional DLN. Nevertheless, in our model where a strong influx of neutrophils was induced, infected mononuclear cells were not observed at early time points in ADLN. Interestingly, Rotta *et al*. recently reported that local inflammation induced by *Salmonella typhimurium* injected into the skin blocked inflammatory monocyte migration and conversion into DCs in the DLN [10].

In humans, BCG reported side-effects include local cutaneous lesions and regional suppurative lymphadenitis [24] , and BCG vaccination often develops as local ulcer leaving a characteristic scar [2]. These observations suggest the involvement of acute inflammatory cells, in addition to a role for tissue-resident cells, in the local response to BCG vaccination. Manufactured BCG vaccines are composed of live bacilli - usually in the range of $4x10^4$ to 10^6 CFUs per dose- and also contain dead bacilli [13] which contribute to the strong local inflammatory reaction. The dose we used in our mouse model induced a similar local reaction characterized by the early recruitment of inflammatory cells. We observed that neutrophils massively infiltrated the dermis after vaccination with BCG. Indeed, neutrophils are acute inflammatory cells that provide the first line of defense against infection. Neutrophils have previously been described as the first cells recruited to tissue following infection with various mycobacterial species [25-28]. We found that neutrophils were recruited to the skin within four hours after intradermal BCG injection and colocalized with bacilli which they efficiently phagocytosed. However, invariably high numbers of bacteria could be grown from the dermis for at least 14 days showing that neutrophils did not efficiently clear BCG in skin. This is consistent with a report that mouse blood neutrophils efficiently phagocytose BCG but that the oxidative burst, essential for killing, is impaired [27]. During the first three days, neutrophils remained mainly concentrated at the injection site where

they focused around BCG. Later after injection, macrophages were localized close to neutrophils suggesting a granuloma-like formation (data not shown). It was recently shown that neutrophils play an essential role in the early granulomatous response in the lung after TB infection in mice [29]. Our study suggests a role for neutrophils in the establishment of this immune cell structure after BCG vaccination as well, although its precise contribution is unknown.

Neutrophils are considered as end-stage inflammatory cells, rapidly recruited to inflammatory sites to fight against microbial infection. There, they are assumed to rapidly die before phagocytosis by resident macrophages. Thus, we were surprised to observe that neutrophils were also the main early BCG host cells in the ADLN. As soon as four hours post-injection, neutrophils colocalized with BCG in the subcapsular space indicating that they had reached the lymphoid tissue via afferent lymph. By using two different fluorescent BCG strains, we observed that neutrophils reaching the ADLN were mainly, although not exclusively, loaded with one color indicating that they had phagocytosed BCG in the periphery. Strikingly, using antibody directed against Lyve-1, a molecule only expressed in lymphatic endothelium [15], we could observe BCG-infected neutrophils in skin lymphatic vessel lumen only a few hours after BCG vaccination thus confirming the migration of infected neutrophils from periphery to the secondary lymphoid organ via afferent lymphatics. So far, such a role in microorganism transport has only been documented for DCs [4,20] and inflammatory monocytes [9]. We report here that neutrophils may also play such a role. Nevertheless, our data do not exclude that bacilli also enter the ADLN as cell-free particles to be phagocytosed there by neutrophils. Despite their high phagocytic capacity and bactericidal functions, neutrophils could not prevent BCG from persisting in the lymphoid tissue. Thus, as recently suggested for *M. tuberculosis* infection in

lungs [30], we think that neutrophils are Trojan horses for intracellular mycobacteria and could also shelter them in the DLN.

We observed that fluorescent-labeled neutrophils injected into the ears, could efficiently reach the ADLN capsular space upon BCG administration. Injection of green neutrophils in the left ear and red neutrophils in the right ear resulted in detection of a single-color fluorescence under the ipsilateral ADLN capsule, excluding their circulation via blood vasculature. Together with the detection of neutrophils in skin lymphatic vessels following BCG inoculation, this provides direct *in vivo* evidence that neutrophils migrate from inflamed skin to the ADLN and thus extend their function beyond the inflamed tissue site.

Early invasion of the DLN by neutrophils migrating from peripheral tissue likely also impact on the T-cell response which is initiated in these immune sites. Neutrophils polarize the Th2 response in mice suceptible to infection with *Leishmania major* suggesting an immunomodulatory function [31]. Mast cells and eosinophils are recruited to the DLN upon sensitization with allergens and may play a direct role in antigen presentation [32,33]. However such a role is controversial for eosinophils that cooperate with local DCs for priming of the T-cell response, rather than functioning as antigen presenting cells by themselves [34]. Early after BCG vaccination, contacts between neutrophils and T-cells as well as DCs were observed in the ADLN (Figure 7B). This suggests that neutrophils, together with T-cells and resident DCs, may play an important role in the mycobacterial antigen presentation process. However, as neutrophils are not highly efficient at degrading BCG, they could also shelter bacilli in the DLN and impair or delay the induction of the adaptive immune response. Taken together, our present findings justify to revisit the role played by neutrophils during BCG vaccination.

Acknowledgements

We are most grateful to Ludovic Tailleux for strong support throughout the work, Pascal Roux and Emmanuelle Perret from the Plate-Forme d'Imagerie Dynamique (Institut Pasteur, Paris) for confocal microscopy and Patricia Charles for technical assistance. We are thankful to Geneviève Milon for teaching us inoculation in mouse ears and constant support and to Daniel Scott for critical reading of the manuscript. We acknowledge David Jackson and Wilbert Bitter for sharing reagents with us.

References

1. Colditz GA, Brewer TF, Berkey CS, et al. Efficacy of BCG vaccine in prevention of tuberculosis. Meta-analysis of the published literature. JAMA. 1994;271:698-702.
2. Fine P, Carneiro I, Milstien J, Clements C. Issues Relating to the Use of BCG in Immunization Programmes. A Discussion Document. Geneva,World Health Organization;1999.WHO publication no. WHO/V&B/99.23.
3. Turville S, Cameron P, Handley A, et al. Diversity of receptors binding HIV on dendritic cell subsets. Nat Immunol. 2002;3:975-982.
4. Moll H, Fuchs H, Blank C, Röllinghoff M. Langerhans cells transport *Leishmania major* from the infected skin to the draining lymph node for presentation to antigen-specific T cells. Eur J Immunol. 1993;23:1595-1601.
5. Rescigno M, Urbano M, Valzasina B, et al. Dendritic cells express tight junction proteins and penetrate gut epithelial monolayers to sample bacteria. Nat Immunol. 2001;2:361-367.
6. Pron B, Boumaila C, Jaubert F, et al. Dendritic cells are early cellular targets of *Listeria monocytogenes* after intestinal delivery and are involved in bacterial spread in the host. Cell Microbiol. 2001;3:331-340.
7. Randolph G, Beaulieu S, Lebecque S, Steinman R, Muller W. Differenciation of monocytes into dendritic cells in a model of transendothelial trafficking. Science. 1998;282:480-483.
8. Geissmann F, Jung S, Littman D. Blood monocytes consist of two principal subsets with distinct migratory properties. Immunity. 2003;19:71-82.
9. Drevets D, Dillon M, Schawang J, et al. The Ly-6C^{hi} monocyte subpopulation transports *Listeria monocytogenenes* into the brain during systemic infection of mice. J Immunol. 2004;172:4418-4424.
10. Rotta G, Edwards E, Sangatelli S, et al. Lipopolysaccharide or whole bacteria block the conversion of inflammatory monocytes into dendritic cells in vivo. J Exp Med. 2003;198:1253-1263.
11. Méderlé I, Bourguin I, Ensergueix D, et al. Plasmidic versus insertional cloning of heterologous genes in *Mycobacterium bovis* BCG : impact on *in vivo* antigen persistence and immune responses. Infect Immun. 2002;70:303-314.
12. van der Sar AM, Musters RJP, van Eeden FJM, Appelmelk BJ, Vandenbroucke-Grauls CMJE, Bitter W. Zebrafish embryos as a model host for the real time analysis of *Salmonella typhimurium* infections. Cell Microbiol. 2003;5:601-611.
13. Gheorghiu M, Lagrange P, Fillastre C. The stability and immunogenicity of a dispersed-grown freeze-dried Pasteur BCG vaccine. J Biol Standard. 1988;16:15-26.
14. Stoitzner P, Holzmann S, McLellan AD, et al. Visualization and characterization of migratory Langerhans cells in murine skin and lymph nodes by antibodies against Langerin/CD207. J Invest Dermatol. 2003;120:266-274.
15. Banerji S, Ni J, Wang SX, et al. LYVE-1, a new homologue of the CD44 glycoprotein, is a lymph-specific receptor for hyaluronan. J Cell Biol. 1999;144:789-801.
16. Belkaid Y, Jouin H, Milon G. A method to recover, enumerate and identify lymphomyeloid cells present in an inflammatory dermal site: a study in laboratory mice. J Immunol Meth. 1996;199:5-25.
17. Romani N, Ratzinger G, Pfaller K, et al. Migration of dendritic cells into lymphatics-the Langerhans cell example : routes, regulation and relevance. Int Rev Cytol. 2001;207:237-271.

18. Dupasquier M, Stoitzner P, van Oudenaren A, Romani N, Leenen P. Macrophages and dendritic cells constitute the main populations in the mouse dermis. J Invest Dermatol. 2004;123:876-879.
19. Fleming T, Fleming M, Malek T. Selective expression of Ly-6G on myeloid lineage cells in mouse bone marrow. RB6-8C5 mAb to granulocyte-differenciation antigen (Gr-1) detects members of the Ly-6 family. J Immunol. 1993;151:2399-2408.
20. Hu J, Gardner MB, Miller CJ. Simian Immunodeficiency Virus rapidly penetrates the cervicovaginal mucosa after intravaginal inoculation and infects intraepithelial dendritic cells. J Virol. 2000;74:6087-6095.
21. King N, Parr E, Parr M. Migration of lymphoid cells from vaginal epithelium to iliac lymph nodes in relation to vaginal infection by Herpes Simplex Virus type 2. J Immunol. 1998;160:1173-1180.
22. Baldwin T, Henri S, Curtis J, et al. Dendritic cell populations in *Leishmania major*-infected skin and draining lymph nodes. Infect Immun. 2004;72:1991-2001.
23. Itano A, McSorley S, Reinhardt R, et al. Distinct dendritic cell populations sequentially present antigen to CD4 T cells and stimulate different aspects of cell-mediated immunity. Immunity. 2003;19:47-57.
24. Lotte A, Wasz-Höckert O, Poisson N, Dumitrescu N, Verron M, Couvert E. BCG complications. Adv Tubercl Res. 1984;21:107-193.
25. Appleberg R, Pedrosa J, Silva M. Host and bacterial factors control the *Mycobacterium avium*-induced chronic peritoneal granulocytosis in mice. Clin Exp Immunol. 1991;83:231-236.
26. Silva M, Silva M, Appleberg R. Neutrophil-macrophage cooperation in the host defence against mycobacterial infections. Microb Pathog. 1989;6:369-380.
27. Seiler P, Aichele P, Raupach B, Odermatt B, Steinhoff U, Kaufmann S. Rapid neutrophil response controls fast-replicating intracellular bacteria but no slow-replicating *Mycobacterium tuberculosis*. J Infec Dis. 2000;181:671-680.
28. Fulton S, Reba S, Martin T, Boom W. Neutrophil-mediated mycobactericidal immunity in the lung during *Mycobacterium bovis* BCG infection in C57/BL6 mice. Infect Immun. 2002;70:5322-5327.
29. Seiler P, Aichele P, Bandermann S, et al. Early granuloma formation after aerosol *Mycobacterium tuberculosis* infection is regulated by neutrophils via CXCR3-signaling chemokines. Eur J Immunol. 2003;33:2676-2686.
30. Eruslanov EB, Lyadova IV, Kondratieva TK, et al. Neutrophil responses to *Mycobacterium tuberculosis* infection in genetically susceptible and resistant mice. Infect Immun. 2005;73:1744-1753.
31. Tacchini-Cottier F, Zweifel C, Belkaid Y, et al. An immunomodulatory function for neutrophils during the induction of a CD4+ Th2 response in BALB/c mice infected with *Leishmania major*. J Immunol. 2000;165:2628-2636.
32. Wang H-W, Tedla N, Lloyd AR, Wakefield D, Patrick McNeil H. Mast cell activation and migration to lymph nodes during induction of an immune response in mice. J Clin Invest. 1998;102:1617-1626.
33. Shi H-Z, Humbles A, Gerard C, Jin Z, Weller PF. Lymph node trafficking and antigen presentation by endobronchial eosinophils. J Clin Invest. 2000;105:945-953.
34. van Rijt LS, Vos N, Hijdra D, de Vries VC, Hoogsteden HC, Lambrecht BN. Airway eosinophils accumulate in the mediastinal lymph nodes but lack antigen-presenting potential for naive T cells. J Immunol. 2003;171:3372-3378.

Legends to figures

Figure 1. BCG bacilli are rapidly detected and persist in ADLN after intradermal vaccination in the ear. BCG (10^6 CFUs) was inoculated into the dermis of each ear dorsum. From 4 hours to 14 days post injection, each ear (closed circles) and ADLN (open circles) were harvested and BCG multiplication was estimated by counting CFUs after plating on selective medium ; data are the mean CFUs ± S.D. from five animals i.e. ten ears and ADLN processed individually.

Figure 2. BCG is neither associated with dendritic cells nor with macrophages in the dermis. (A) From 4 to 72 hours after BCG-*egfp* inoculation, skin explants cells were stained with CD11c and analyzed by flow cytometry. (B) Ear cryosections from BCG-*egfp* and mock-injected mice were immunostained with antibodies directed against CD11c and mMGL a receptor largely distributed among dermal phagocytes. Co-localization of BCG (green) with these cell populations (red) could not be observed (magnification x200).

Figure 3. Dendritic cells do not carry BCG into the ADLN after vaccination in the ear dermis. (A) Low-density cells recovered from ADLN from 4 to 72 hours after BCG-*egfp* injection were stained with anti-CD11c and analyzed by flow cytometry (B) ADLN sections from BCG or mock-injected mice were immunostained with anti-CD11c. At 72 hpi, co-localization of conventional DCs and BCG was observed on rare occasions (see insert shown at magnification x400) but most of the bacilli remained localized under the ADLN capsule (magnification x100)

Figure 4. Neutrophils are rapidly recruited to the dermis where they phagocytose BCG and then massively crawl out from the skin. (A) Cells crawling out from ear skin explants from 4 to 72 hours after BCG-*egfp* vaccination, were analyzed by flow cytometry after CD11b staining. (B) Twenty-four hours after vaccination, $EGFP^+$ gated skin explant cells were phenotyped as $CD11b^+$ $Ly\text{-}6G^+$, $MHCII^-$ and $F4/80^-$. (C) $CD11b^+/EGFP^+$ cells were sorted by flow cytometry and observed by light microscopy after staining with May-Grümwald Giemsa. Characteristic polylobed nuclei confirmed that main BCG-host cells in skin are neutrophils. In most cases, several bacilli were detected inside each neutrophil (arrows). (D) Ear-skin cryosections were immunolabeled with anti-Ly-6G (red) (magnification x100). Neutrophils that invaded the dermis from 4 hpi to 72 hpi were focally organized around bacilli at the injection site. At 12 hpi bacilli (green) and neutrophil (red) colocalization was observed by confocal microscopy (apochromate objective x 63 (N.A. : 1.4)).

Figure 5. Neutrophils massively infiltrate ADLN early after vaccination and shelter BCG. (A) Twenty four hours after vaccination with BCG-*egfp*, ADLN $EGFP^+$ gated cells were phenotyped as $CD11b^+$, $Ly\text{-}6G^+$, $F4/80^-$ and $MHCII^-$ indicating they were neutrophils. (B) $CD11b^+$ ADLN cells were magnetically enriched and $EGFP^+$ cells were FACS sorted. The majority of the $CD11b^+/EGFP^+$ cells were positive for Ly-6G (red), and microscopy analysis revealed their characteristic polylobed nucleus stained with DAPI (blue). Several bacilli (green) were often detected inside the same neutrophil. (C) Neutrophil recruitment to the ADLN was analyzed at 4, 12, 24 and 72 hpi after BCG-*egfp* injection, by immunostaining cryosections with anti-Ly-6G. From 4 to 24 hpi, neutrophils (red) massively infiltrated the subcapsular space and sinuses of the ADLN and mainly colocalized with BCG (green). Bacilli were detected inside

neutrophils under the ADLN capsule as observed by confocal microscopy (apochromate objective x 63 (N.A. : 1.4)). At 72 hpi, neutrophils disappeared from the ADLN (magnification x100).

Figure 6. Infected neutrophils leave the skin via afferent lymphatics after BCG injection and shuttle fluorescent bacilli to the ADLN. (A) 10^6 CFUs of rBCG-*dsred* and rBCG-*egfp* fluorescent strains were injected into two adjacent distinct sites of the ear dorsum (left panel). Four hours later, ADLN cryosections were laser scanned under a confocal microscope to colocalize red or green bacilli with Ly-6G$^+$ cells (blue). Neutrophils carrying either red or green bacilli or co-infected with both strains in the ADLN were scored in seven fields from two ADLN sections. Right panel : control co-injection of mixed red and green bacilli in the same site (apochromate objective x 63 (N.A. : 1.4)). (B) Four hours after BCG-*egfp* inoculation, ear sections were immunostained with anti-Lyve 1 (brown) and neutrophils were detected either by counterstaining polylobed nuclei with hematoxylin or by anti-Ly-6G (blue). Neutrophils were detected inside the lumen of lymphatic vessels in the injection site vicinity. (C) Four hours following BCG-*egfp* inoculation, ear dermis was stained with anti-Lyve 1 (red) and anti Ly-6G (blue), and a three dimensional 'orthogonal' slice projection was analyzed by confocal microscopy. The large central panel shows a single image among 46 slices recorded at 0.23 µm intervals. To characterize cells inside lymphatic vessels (underlined by red dashes), x-axis (green line) and y-axis (red line) were defined for sliced z-axis reconstruction. The corresponding results for the x,z slice and y,z slice are shown and the crossing point between green and red lines represents the z-stack position of the central panel image. (apochromate objective x 63 (N.A. : 1.4)). A neutrophil carrying bacilli inside the lymphatic vessel lumen is depicted.

Figure 7. Fluorescent labeled neutrophils accumulate in the ipsilateral ADLN and reach the paracortical region. (A) Bone-marrow neutrophils were labeled with CFSE (green) or PKH26 (red), and injected inside the left or right ear dorsum concomitantly with 10^6 CFUs of wild type BCG (upper panel). Four hours later, green neutrophils were detected only in the left ADLN and red neutrophils in the right ADLN (middle panel). In three independent experiments analyzed, no mixed green and red neutrophils were ever observed. Control mock-injection induced only moderate infiltration of fluorescent neutrophils in the regional ADLN (lower panel) (magnification x100). (B) At 12 hpi, Ly-6G$^+$ neutrophils (green) were detected inside the T-cell (CD4$^+$ and CD8$^+$ in red) area of the ADLN (left panel). CD11c$^+$ (red) DCs were also detected in the same zone and contacts between neutrophils and DCs could be observed (right panel, arrows, magnification x100)

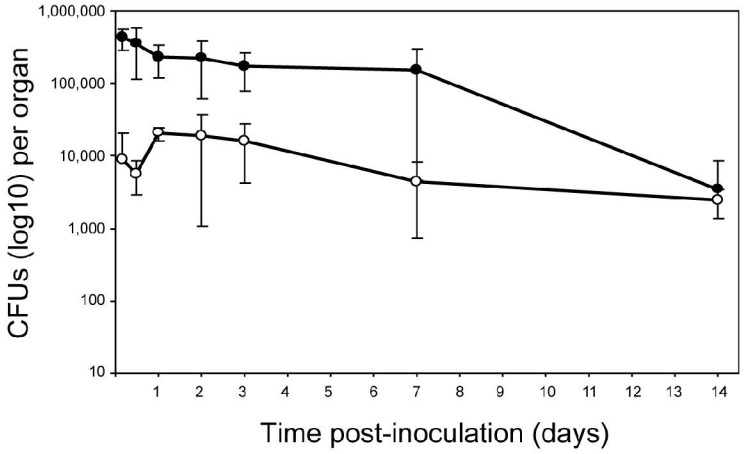

ABADIE *et al.*, Figure 1

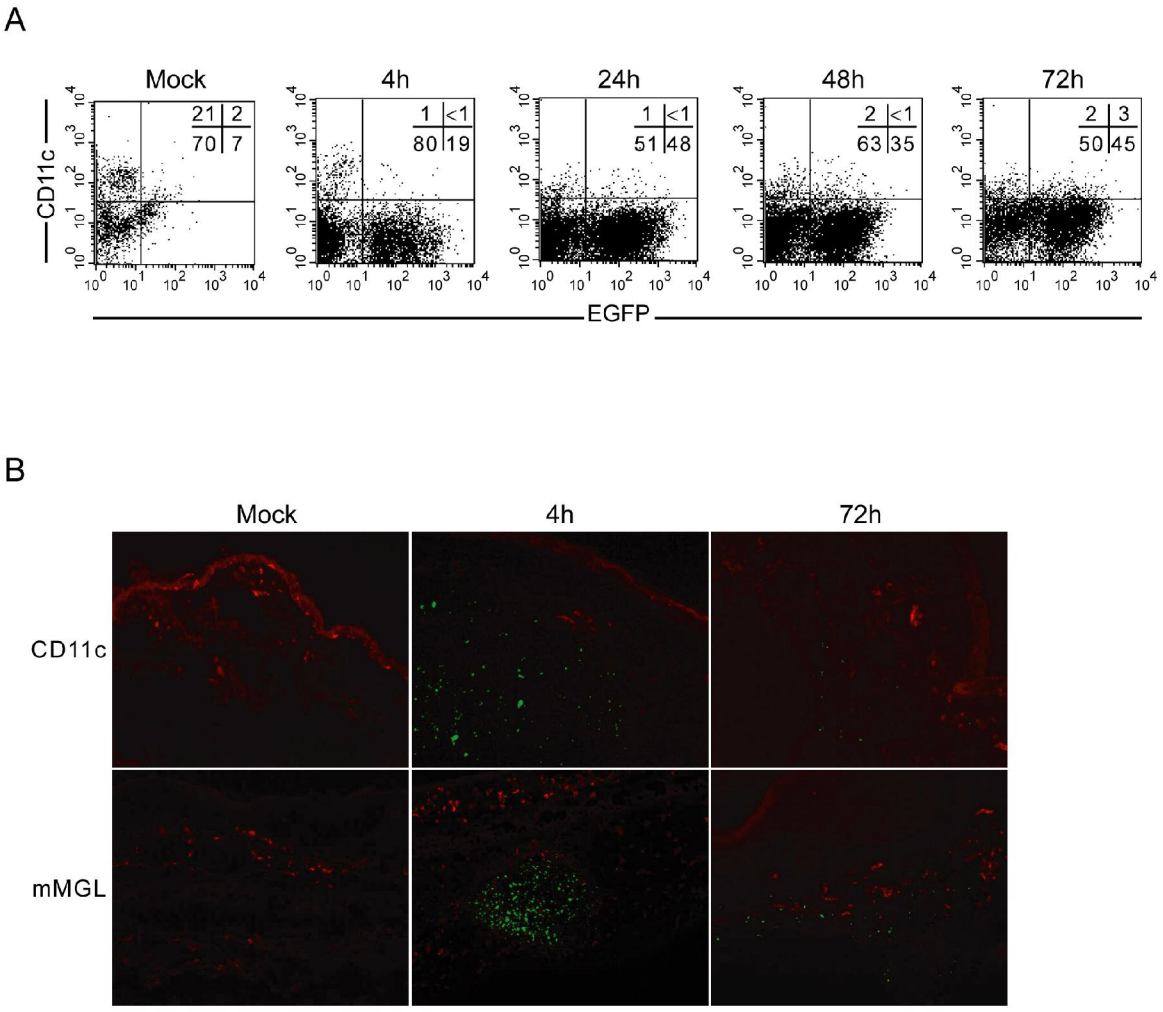

ABADIE *et al.*, Figure 2

A

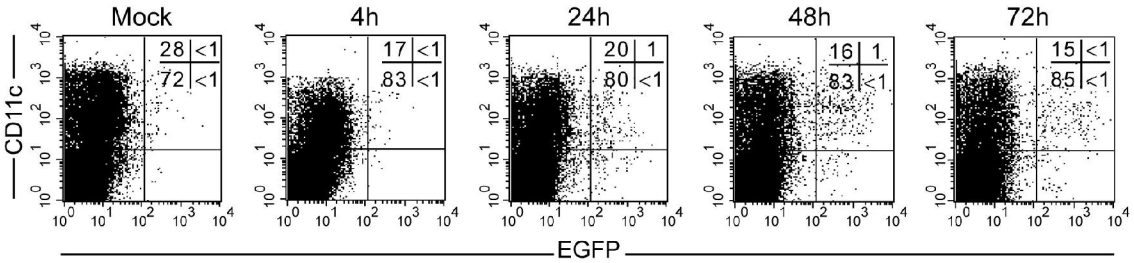

B

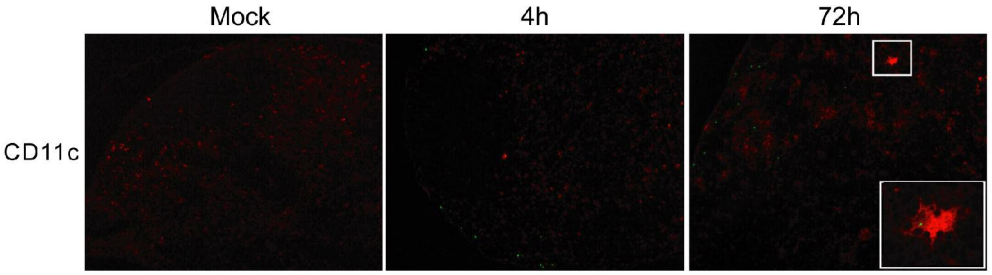

ABADIE *et al.*, Figure 3

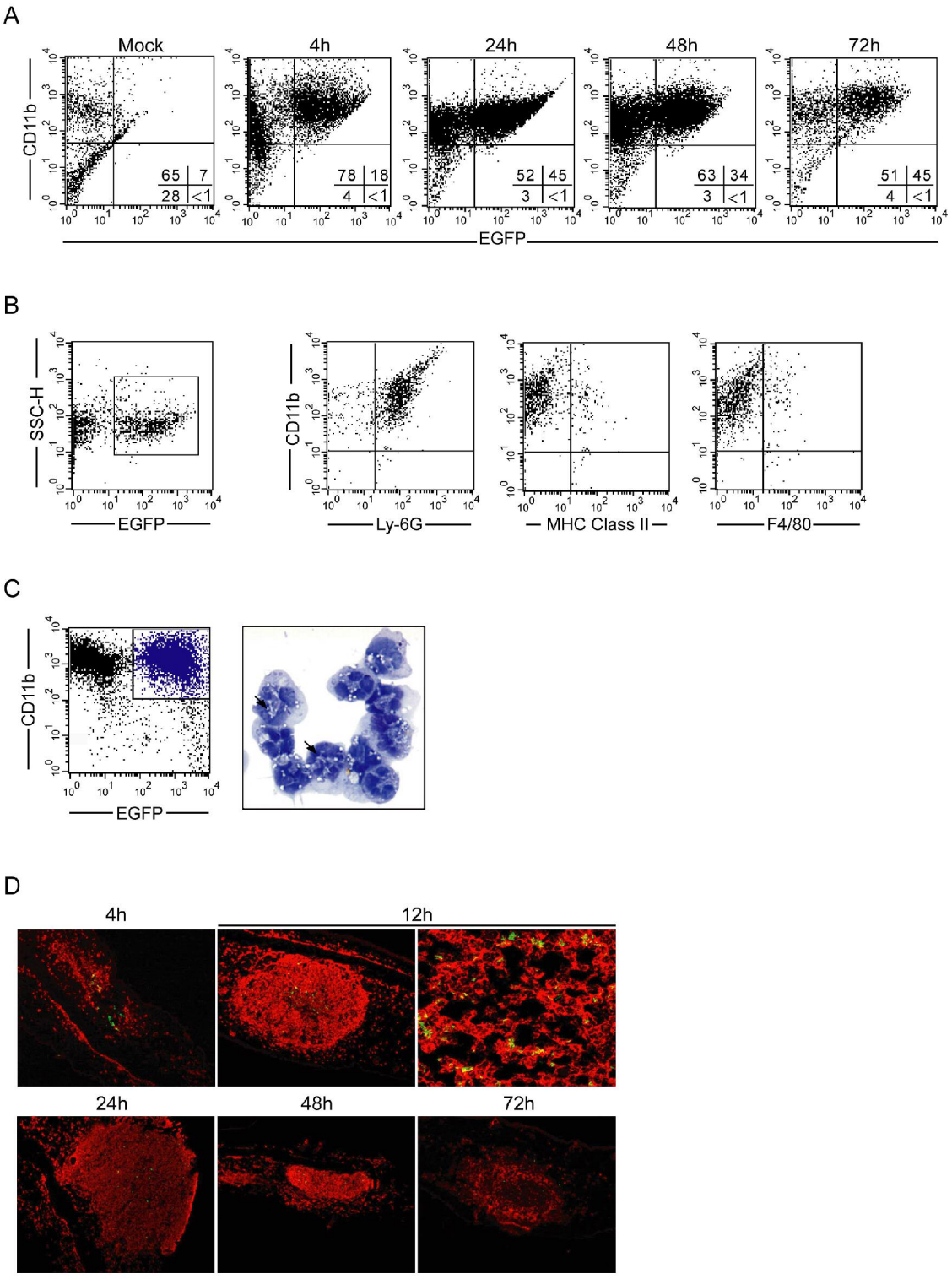

ABADIE *et al.*, Figure 4

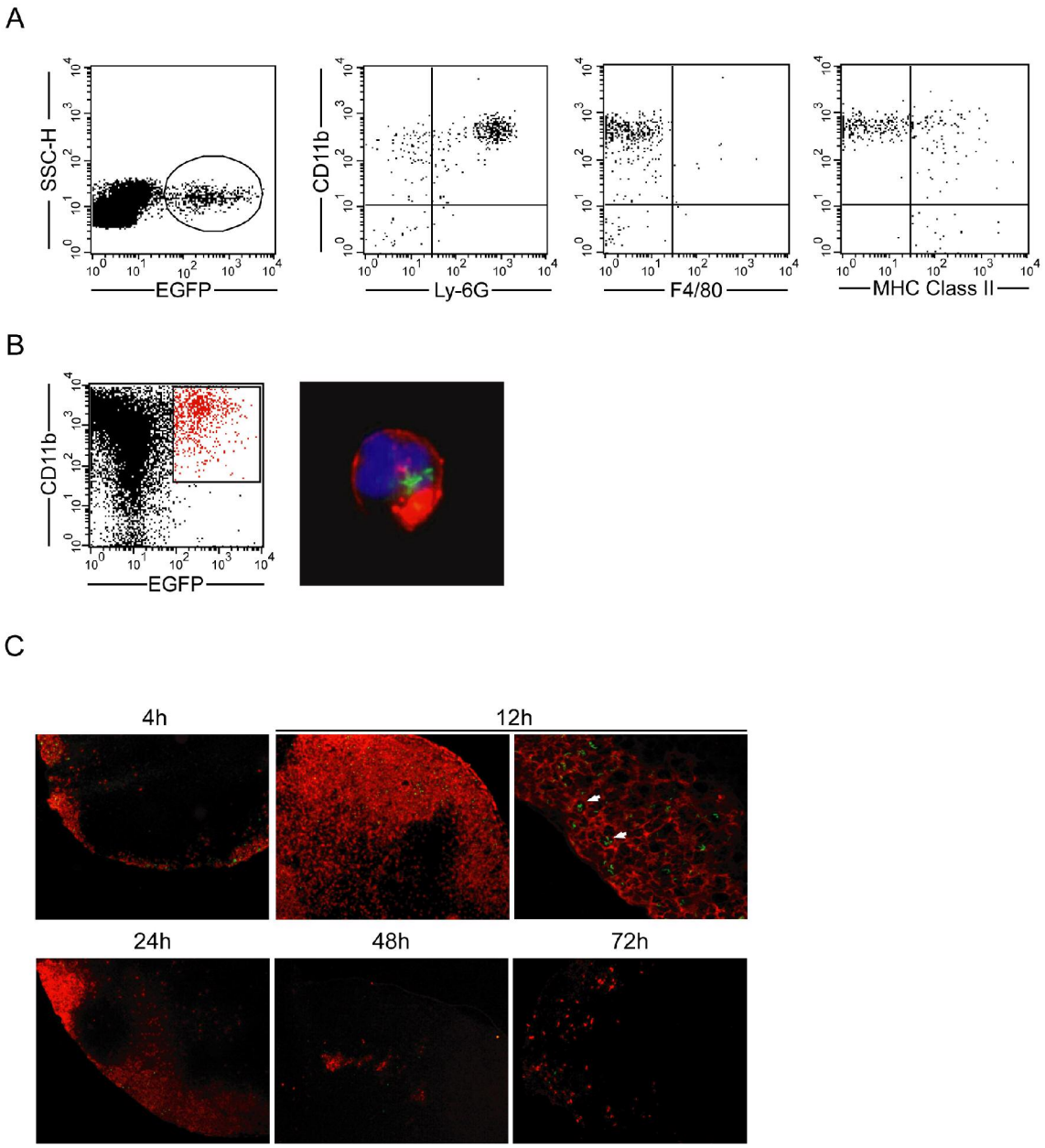

ABADIE *et al.*, Figure 5

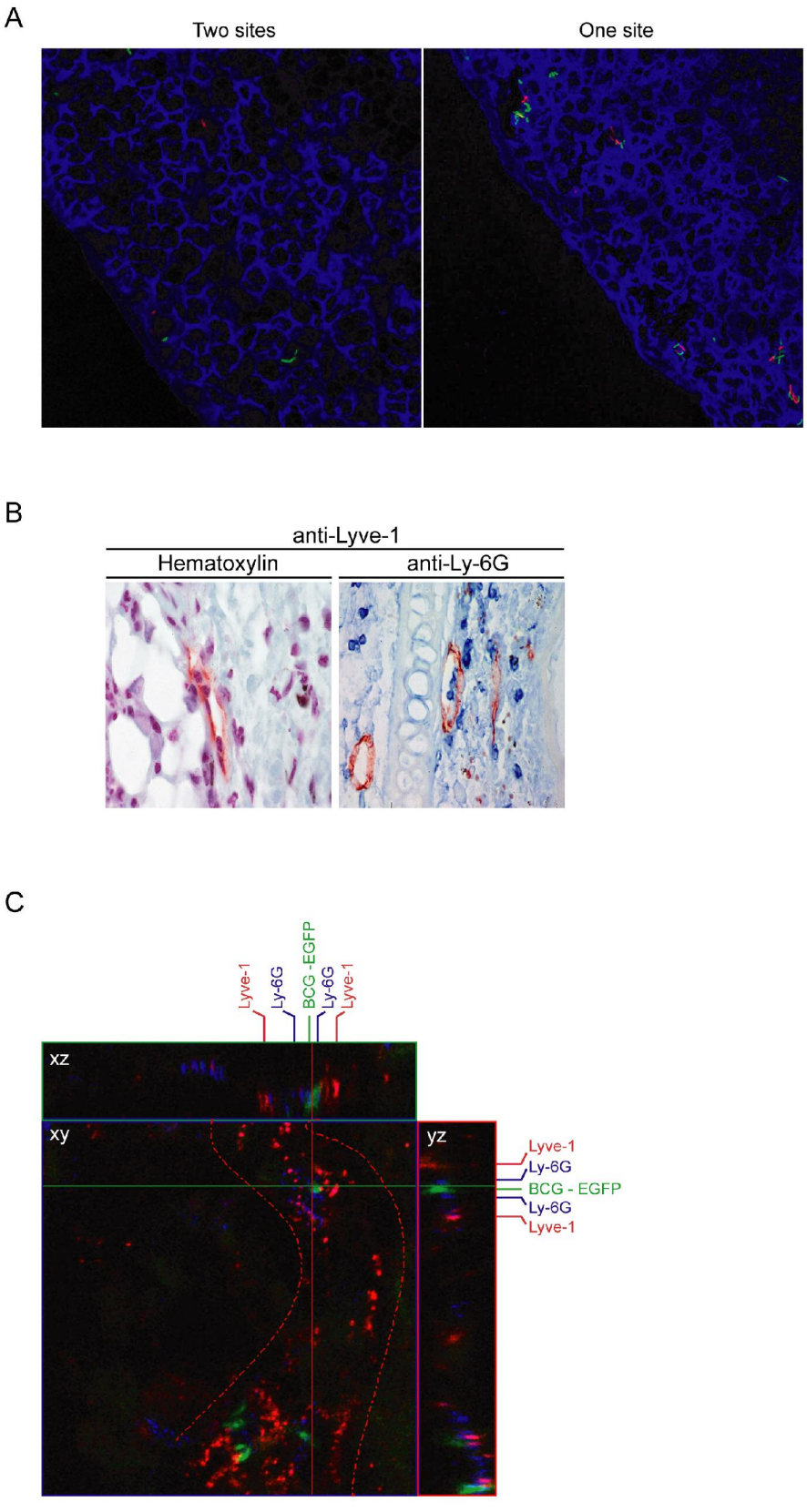

ABADIE *et al.*, Figure 6

A

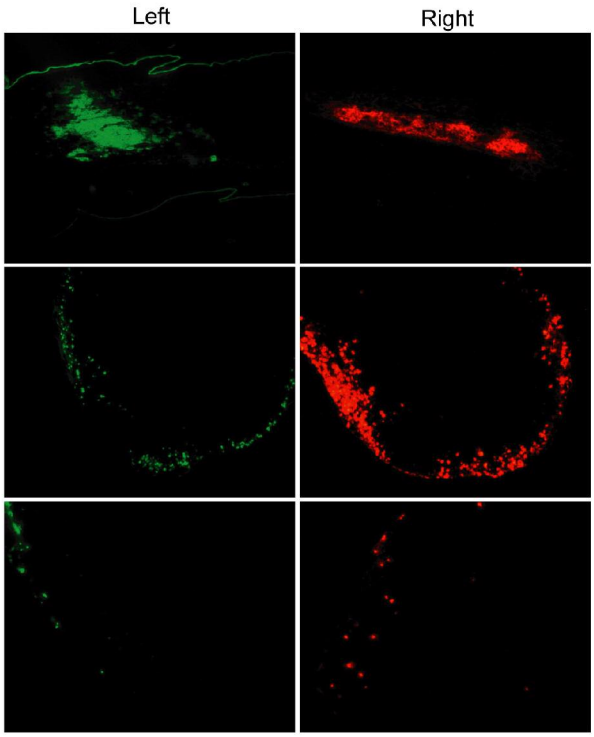

B

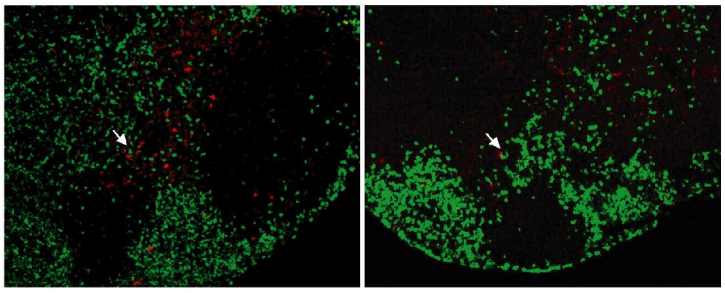

ABADIE *et al.*, Figure 7